

X-ray-absorption near-edge structure of alkali halides: The interatomic-distance correlation

M. Kasrai

Department of Chemistry, The University of Western Ontario, London, Ontario, Canada N6A 5B7

M. E. Fleet

Department of Geology, The University of Western Ontario, London, Ontario, Canada N6A 5B7

G. M. Bancroft

Department of Chemistry, The University of Western Ontario, London, Ontario, Canada N6A 5B7

K. H. Tan and J. M. Chen

Canadian Synchrotron Radiation Facility, University of Wisconsin, Stoughton, Wisconsin 53589

(Received 16 August 1990)

Cl L -edge x-ray-absorption near-edge-structure (XANES) total-electron-yield spectra have been recorded for LiCl, NaCl, KCl, as well as NaCl-KCl solid solutions, in the region of 190–280 eV, using synchrotron radiation. The spectra are interpreted using a model previously developed and based on a $1/R^2$ correlation. All post-edge features may be correlated with interatomic distances and lattice spacings. The model also assigns the XANES features to interatomic distances and lattice spacings in Na and F K -edge spectra of alkali halides.

I. INTRODUCTION

The Cl $L_{2,3}$ x-ray-absorption near-edge-structure (XANES) spectra for alkali chlorides have been reported in several studies.^{1–6} Sagawa and co-workers^{1–3} studied the Cl L -edge spectra in the series from LiCl to CsCl, both at 80 K and room temperature. They interpreted the first ~ 13 eV of the spectra in terms of the transitions to core excitons as well as the conduction band, using band-structure calculations by Kunz.⁷ Brown *et al.*⁴ also investigated the Cl L edge of alkali chlorides along with other soft x-ray-absorption edges. Their results are in good agreement with Sagawa's work, but differ in interpretation using the same band-structure calculations. Watanabe⁵ investigated the Cl L -edge spectra of solid solutions of alkali chlorides. In general, the interpretation of the first ~ 15 eV of the XANES spectra using a band-structure calculation has not been very successful, due to the uncertainty of the edge position and to lack of inclusion of the exciton transitions. Pantelides and Brown⁶ have determined the edge positions for several alkali halides using XPS and band-gap values in an attempt to correlate the band structure findings with the absorption data. Extensive band structure calculations have been performed for alkali halides mostly by Kunz and co-workers⁸ whose latest calculation seems to agree with the photoemission data⁹ but fails to account for the photoabsorption findings. This is believed to be due mainly to the exclusion of core-exciton transitions.⁸ Vedrinskii *et al.*¹⁰ have applied cluster calculations in the framework of multiple scattering in order to explain the K and $L_{2,3}$ edge spectra of KCl. More recently Fujikawa and co-workers¹¹ have applied full multiple-scattering calculation to interpret the XANES features of the Na K edge of NaCl and alkali-chloride mixed crystals.

At present, no comprehensive theory is available for the interpretation of the entire range of Cl L -edge XANES spectra of alkali chlorides. In this study we apply a simple approach which was used for the sulfur L edge¹² to correlate the XANES features (~ 10 – 50 eV above the edge) with interatomic distances.

II. EXPERIMENTAL

All chemicals used were of analytical grade. Alkali chlorides were in the form of either powder or fused crystals. The powder samples were carefully dried at 110° C and further dried in the vacuum chamber before analysis. The fused samples were used in the form of ingots. No difference was found in the spectra of powders and fused samples. Starting compositions for (Na,K)Cl solid solutions were melted at 900° C for 2 h in a platinum crucible with a well fitting lid. Prescribed amounts were melted under vacuum in small (10×5×3 mm) platinum dishes, sealed in silica-glass tubes, annealed at 630° C for 2 h, and quenched in cold water.¹³ Homogeneity was confirmed by x-ray-diffraction analysis, but the solid solutions were very unstable when exposed to air. Therefore, samples were transferred to the total electron yield (TEY) spectrometer in a dry nitrogen glove bag. The surface of one fused sample was cleaned by Ar⁺ sputtering to investigate the possibility of surface contamination. The spectra obtained before and after the sputtering were identical. Thus other samples were used without any surface treatments. The x-ray-absorption spectra were obtained at the Canadian Synchrotron Radiation Facility (CSRF),¹⁴ University of Wisconsin, at room temperature. The radiation was monochromatized with a Mark IV Grasshopper monochromator with the energy resolution of ~ 0.4 eV at 200 eV. The photoabsorption spectra were

taken, in the region of 190–280 eV, by recording the total electron yield in the analog mode from the sample as a function of energy. The details of the technique have been reported elsewhere.¹² At least three spectra were combined digitally and background was subtracted using the BAN computer program.¹⁵ The monochromator was calibrated using known edges.¹⁶ This calibration gave the first sharp peak of elemental sulfur at 165.0 eV. All spectra were calibrated using the sulfur peak which is close to the Cl *L*-edge absorption lines.

III. RESULTS and DISCUSSION

A. General features of XANES spectra

The XANES region of the absorption spectra is rich in structure that is sensitive to the local symmetry and electronic environment as well as the bond distances of the absorbing atom.^{17,18} LiCl, NaCl, and KCl all have NaCl-type crystal structures, with the alkali metal coordinated to six Cl, and a cubic face-centered (fcc) lattice, whereas the CsCl structure has Cs coordinated to eight Cl and a cubic primitive lattice. Figure 1 shows the total electron yield Cl *L*_{2,3} edge spectra of LiCl, NaCl, and KCl and Fig. 2(a) shows the spectrum of CsCl. The peak positions for all alkali chlorides studied are given in Table I and compared with literature values.^{2,4} To our knowledge this is the first total electron yield XANES report of the alkali chlorides. All previous studies have been performed in the absorption mode using thin films.^{1–5} Overall, our spectra are similar to the spectra obtained by Iguchi *et al.*² and Brown *et al.*⁴ measured in the absorption mode at room temperature. Indeed, peak positions agree very closely to the previously reported values when corrected for slight differences in calibration. In general, the spectra [Figs. 1(a)–1(c)] consist of several sharp features (*a–e*) followed by rather broad peaks

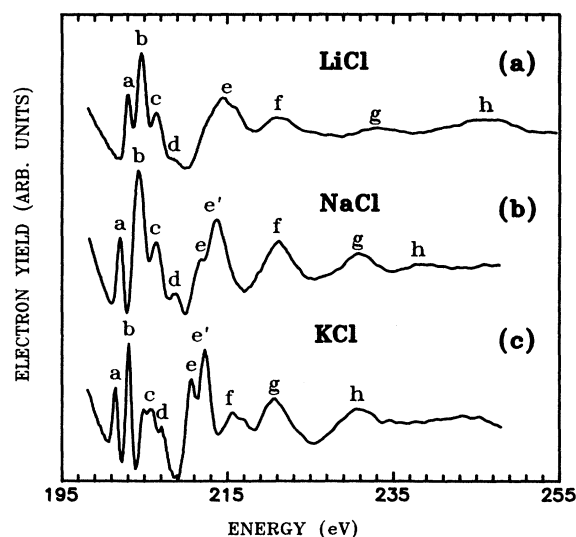


FIG. 1. Chlorine *L*-edge XANES spectra of alkali chlorides: (a) LiCl; (b) NaCl; (c) KCl.

(*f–h*). Moving from LiCl to KCl in the sequence of increasing unit-cell parameter, the features become sharper and shift towards the low-energy end of the spectrum. Also, some of the peaks such as *e* and *c* begin to resolve into doublets. CsCl, having a different structure from other alkali chlorides studied, has a somewhat different XANES spectrum [Fig. 2(a)]; the relative intensities in the first part of the spectrum (*a–e*) are different and the peaks are not as well resolved.³

In order to investigate a XANES spectrum we divide it into two regions. The edge region (to about 13 eV), covering peaks *a–e*, is believed to be due to the transition of photoelectrons to unoccupied bound states as well as the density of states maxima in the conduction band; whereas the post-edge region (to about 45 eV) encompassing peaks *e–h* results from single and multiple scattering of photoelectrons with nearest-neighbor and extended-neighbor atoms.^{17,18}

B. Edge region

Many theoretical studies in the past have concentrated on interpretation of the first few peaks (*a–d*) of the absorption spectra using band-structure calculations.^{7,8} Because of the difficulty in calculating the absolute transition energies, the energy scale of the density of states has been moved arbitrarily in order to get a reasonable correspondence between theoretical and experimental peaks. For this reason peak *a* has sometimes been assigned to an excitonic transition³ with a hole in the *2p* level of chlorine and sometimes to a transition to states in the conduction band.⁴ Pantelides and Brown⁶ have used x-ray photoelectron spectroscopy (XPS) and optical band-gap data to calculate the position of the conduction

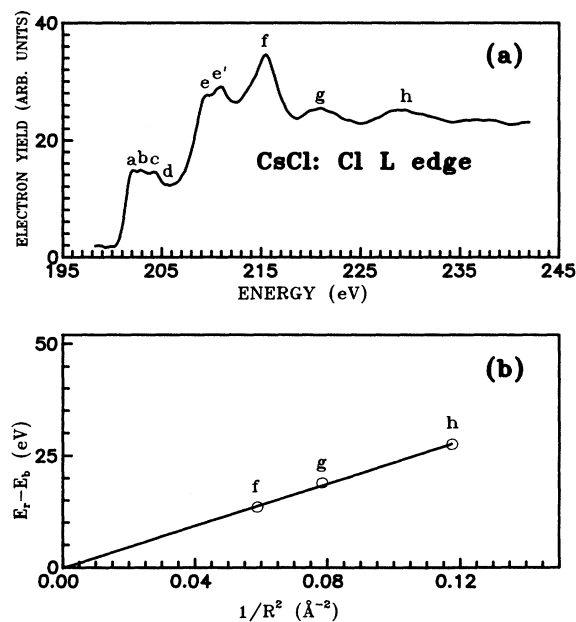


FIG. 2. (a) Chlorine *L*-edge XANES spectrum of cesium chloride; (b) correlation plot between energy and $1/R^2$ for CsCl.

TABLE I. Positions of major peaks (± 0.3 eV) of Cl L -edge absorption spectra of alkali chlorides.

Reference	Peak positions								
	<i>a</i>	<i>b</i>	<i>c</i>	<i>d</i>	<i>e</i>	<i>e'</i>	<i>f</i>	<i>g</i>	<i>h</i>
	LiCl								
This work	203.6	204.7	206.5	208.6	215.0		221.0	233.0	246.1
Iguchi ^a	203.2	204.8	206.5	208.5	215.6		221.5	232.3	246.7
	NaCl								
This work	202.1	204.3	206.4	208.6	211.9	213.8	221.3	230.8	237.9
Iguchi ^a	201.8	204.1	206.1	208.4	211.5	213.6	221.6	230.0	237.6
Brown ^b	201.5	203.6	205.5	208.3	211.8	212.5			
	KCl								
This work	201.5	203.1	205.3	207.1	210.7	212.3	215.7	220.7	230.6
Iguchi ^a	201.6	203.0	205.2	207.0	210.5	212.5	216.4	221.0	230.0
Brown ^b	200.6	202.0	205.0		209.2	211.0	214.2	219.2	228.4
	CsCl								
This work	202.1	202.8	204.2	205.5	209.5	210.9	215.5	221.0	228.8
Iguchi ^a	201.8	202.8	203.7	206.0	209.7	211.5	215.9	221.7	228.6

^aReference 2.^bReference 4.

band edge with respect to the core levels. This approach has been applied to several alkali halides in order to correlate the theoretical findings with the absorption spectra. As a result it was shown that for alkali chlorides, at least, the first peak *a* lies below the conduction band and must be due to a core-exciton transition and not to the transition to the conduction band. This confirmed the original suggestion by Aita *et al.*³ and Watanabe.⁵ It has also been suggested by Watanabe,⁵ who studied solid solutions of alkali chlorides, that the first two spin-orbital coupling pairs *a* and *b* separated by ~ 1.6 eV are indeed attributable to exciton transitions. The other features below 210 eV (*c* and *d*) are interpreted in terms of transitions to band density maxima. However, in the recent calculation by Kunz,⁸ no attempt has been made to correlate the x-ray-absorption spectra with the theoretical findings. Kunz states that, for the L edge, much of the absorption strength initiates from exciton absorption and this effect had not been included in the band calculation.

Looking more closely at the spectra, in particular the KCl spectrum [Fig. 1(c)], one notices a sharp rise in the absorption above 210 eV and the pattern of the spectrum in the region of 202–210 eV appears to repeat itself. This behavior has led previous investigators² to speculate that the structures above 210 eV might be due to the two-electron excitation, that is, the simultaneous excitation of an electron from a Cl $2p$ level and a valence electron from $3p$. However, theoretical calculation¹⁹ has shown that the absorption cross section close to 210 eV is too large to be accounted for entirely by a two-electron excitation and therefore an alternative interpretation has been forwarded. It has been suggested that as in atomic spectra,²⁰ the feature can be interpreted in terms of the delayed band of the $p \rightarrow d$ transition.^{3,5}

In summary, there presently is no overall agreement on interpretation of the x-ray-absorption spectra using the

band-structure calculations. However, it is well established that, based on experimental evidence and the position of the conduction band, peak *a* and its spin-orbit coupling partner peak *b*, and possibly peaks *c* and *d* in the same way, originate from core excitons. But the origin of the other higher-energy features, and in particular the broadbands such as *f* and *g*, is not known at the present time. A theoretical model proposed by Natoli,²¹ suggests that the absorption features above the ionization edge are due to the multiple scattering of photoelectrons by neighboring atoms. Recently, we have developed a model¹² based on Natoli's theory to correlate the XANES features in the S $L_{2,3}$ -edge spectra with interatomic distances in sulfide minerals. We presently use this model to interpret the origin of the features above 210 eV of the Cl $L_{2,3}$ -edge spectra.

C. Post-edge region and interatomic-distance correlation

In contrast to extended x-ray-absorption fine-structure (EXAFS) features, the origin of the post-edge features in the XANES spectra is not well understood.¹⁷ Natoli's theoretical model²¹ based on the multiple scattering of photoelectrons by neighboring atoms has had partial success in correlating near-edge features to interatomic distances. Bianconi and co-workers²² correlated the nearest-neighbor distance in a series of $3d^0$ compounds, including Ti^{4+} , V^{5+} , and Cr^{6+} (all tetrahedrally coordinated to oxygen) with a broad peak in the K -edge XANES spectrum of the metals. This simple approach has been further extended to other transition metals by Lytle and co-workers.¹⁸ In the case of NiO, which has the NaCl structure, they were able to identify and assign the Ni K -edge features to long-range interatomic distances up to the fourth coordination sphere.¹⁸

In our recent investigation of S L -edge XANES spectra of sulfide minerals, including ZnS, MoS₂, and PbS, we

were able to assign all the peaks between 10 and 45 eV above the edge to interatomic distances using a model based on that of Natoli.¹² It was of great interest to further investigate the applicability of this model to other crystalline substances with simple crystal structures using different L edges, and alkali chlorides were chosen for this reason. It was shown by Natoli²¹ that the energy of an absorption peak above the threshold is inversely proportional to R , the distance from the absorbing atom to a neighboring atom, according to the following equation:

$$(E_r - E_b)R^2 = C, \quad (1)$$

where E_r is the energy of the peak of interest, E_b is the energy of a bound or excitonic resonance just before the onset of the edge, and C is a constant for the absorbing material. It can be shown²³ that for a free electron the value of $C = 150.4 \text{ eV \AA}^2$. But in practice C is determined by fitting the experimental data to Eq. (1). In our previous report we showed that Eq. (1) could be used not only to assign the resonance of the nearest neighbor, but it could be applied also to several coordination shells beyond the first shell.¹²

In order to apply Eq. (1) to alkali chlorides, we first determine an approximate value of E_b for each spectrum. As noted above, E_b corresponds to a bound state or excitonic resonance. From the discussion of the previous section it is now well established that peak a , present in all four spectra (Figs. 1 and 2), lies below the edge and is attributable to an excitonic transition. Since the value of C is unknown, the peaks corresponding to different shells have to be located by inspection. It is obvious from the $1/R^2$ relationship in Eq. (1) that the shorter the interatomic distance, the higher the energy of the associated resonance and, consequently, the further from the edge, the absorption peak. Therefore recognizing that XANES

features diminish $\sim 50 \text{ eV}$ above the edge, one can locate the peak corresponding to the first nearest-neighbor shell in the region of 30–50 eV above the edge. Once the first absorption peak is correctly correlated to the first neighbor shell, the other correlations follow in sequence. For the spectra in Fig. 1, features below 260 eV (extending to $\sim 50 \text{ eV}$ above the edge) were correlated qualitatively with interatomic distances calculated using program BADTEA (Ref. 24) and unit-cell parameters of the pure alkali chlorides. It was found that, as in the case of S L -edge work,¹² it was essential to include the lattice spacings (d_{hkl} spacings) in the correlation in order to account for all the peaks in the post-edge region of the XANES spectra. By Eq. (1) and for single-scattering processes, resonance occurs when the photoelectron wavelength $\lambda = R_n$. In applying this theory to the S L -edge spectra of simple sulfides,¹² it was apparent that one prominent absorption peak in each spectrum was unassigned. However, whereas the distance parameter of the unassigned peak did not correspond to a possible interatomic distance it was equivalent to a possible lattice spacing (d_{hkl}). Thus, this earlier study demonstrated the backscattering of photoelectrons by crystal lattice planes. The absorption of backscattered photoelectrons occurs not only when $\lambda = R_n$ but also when $\lambda = d_{hkl}$. The present study further confirms this conclusion. However, we have yet to make observations on corresponding crystalline and

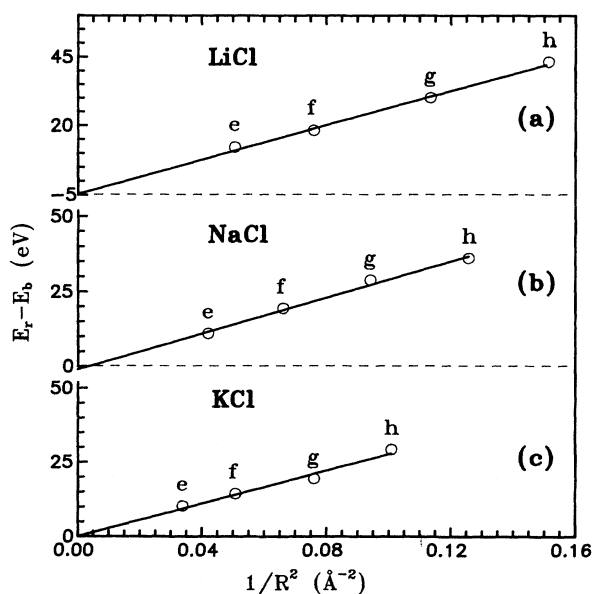


FIG. 3. Correlation plots between energy and $1/R^2$ for Cl L -edge XANES in alkali chlorides: (a) LiCl; (b) NaCl; (c) KCl.

TABLE II. Peak assignments and interatomic distances for L edges.

Shell	Peak	$E_r - E_b$ (eV)	R (Å) Calc.	R (Å) Present
LiCl (Cl L edge)				
R_1	h	43.1	2.57	2.55
d_{111}	g	30.0	2.97	3.00
R_2	f	18.0	3.63	3.70
R_3	e	12.0	4.45	4.32
NaCl (Cl L edge)				
R_1	h	35.8	2.82	2.85
d_{111}	g	28.6	3.26	3.18
R_2	f	19.2	3.89	3.85
R_3	e	10.8	4.88	5.02
KCl (Cl L edge)				
R_1	h	29.1	3.15	3.08
d_{111}	g	19.2	3.63	3.79
R_2	f	14.2	4.44	4.41
R_3	e	10.0	5.45	5.26
CsCl (Cl L edge)				
d_{110}	h	27.5	2.92	2.93
R_1	g	18.9	3.57	3.52
R_2	f	13.4	4.12	4.18
Crystalline Ar (L edge)				
d_{111}	g	17.4	3.07	3.06
R_1	f	11.4	3.75	3.78
R_2	e	6.0	5.31	5.21

amorphous materials. Although we have recognized lattice resonances only in the XANES region, we predict that the higher energy resonances associated with shorter d_{hkl} (and longer reciprocal lattice spacings) extend through the EXAFS region as well, and are obscured by the general EXAFS oscillation and Cl L_1 -edge features.

Figures 3 and 2(b) show plots of $1/R^2$ versus energy and Table II summarizes the results of the correlations and compares interatomic distances derived from Eq. (1) with calculated values. In this correlation the plots pass through zero except for the LiCl one which has an intercept of ~ -5.0 eV with the y axis. Looking at these figures and Table II we notice that the correlation for LiCl, NaCl, KCl, and CsCl is remarkably good and the agreement between the calculated and derived distances is within 0.1 \AA . For CsCl (primitive lattice), the lattice resonance associated with d_{110} is the highest energy absorption peak in the XANES region (and is therefore assigned to peak h), and the resonance associated with d_{100} coincides with R_2 . The values of C calculated from the slope of the plots in Figs. 3 and 2(b) for LiCl, NaCl, KCl, and CsCl are 311, 300, 276, and 237 eV \AA^2 , respectively. The value of C systematically decreases as we move from LiCl to CsCl. This is possibly due to the change in the phase shift of the backscatterer. The available data (Lytle *et al.*,¹⁸ Kasrai *et al.*,¹² Natoli,²¹ present study) suggest that C departs markedly from the free-electron value for ligand absorber atoms. We tentatively attribute this to a change in the phase shift during backscattering, which modifies the effective scattering length.

As a comparison, we are presenting the total electron yield S L -edge XANES spectrum and the correlation plot¹² for PbS (galena) in Fig. 4. PbS has the NaCl struc-

ture and its spectrum can be compared directly with that of NaCl. As expected, the low-energy regions of the two spectra (Figs. 1 and 4) extending to ~ 12 eV above peak a are not similar. This is due to the fact that the conduction band structures for the two compounds are different. PbS is a semiconductor whereas NaCl is an insulator. On the other hand the regions comprising peaks f – h in both spectra are very similar indicating the validity of $1/R^2$ correlation.

It is important to point out that the present correlation of $(E_r - E_b)$ with $1/R^2$ is not fortuitous. As an example, in Fig. 5 a different approach has been taken for the correlation plot for NaCl. In Fig. 5(a) the d_{111} spacing has been excluded from the correlation while in Fig. 5(b) a shorter d_{hkl} spacing ($d_{220} = 1.99 \text{ \AA}$) has been included. Clearly, these correlations are not linear and they do not pass through the origin. Points g and f in Fig. 5(a), and points g and e in Fig. 5(b) deviate from the expected values by as much as 0.5 \AA compared to 0.1 \AA when the suggested correlation is used (see Table II). We have tried many other combinations of d_{hkl} spacings and interatomic distances and all yielded unsatisfactory correlations.

We have also investigated if any of the peaks in the present XANES spectra represent oscillation in the cross section for diffraction of photoelectrons.^{23,25} Using $kR = 2\pi$ and assuming free electron scattering,²² peak positions corresponding to a second oscillation either lie above 50 eV from the edge (for shorter interatomic distances) or do not correspond to any of the observed peaks. Second oscillations are even further extended from the edge with $C \sim 300 \text{ eV \AA}^2$.

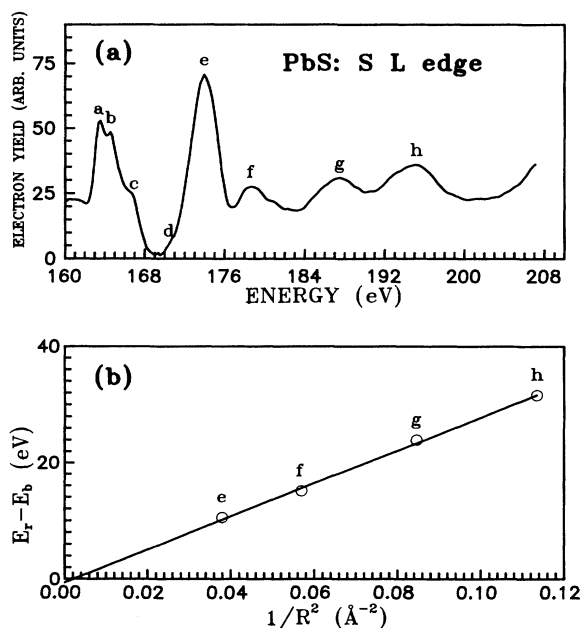


FIG. 4. (a) Sulfur L -edge XANES spectrum of PbS (galena); (b) correlation plot between energy and $1/R^2$ for PbS.

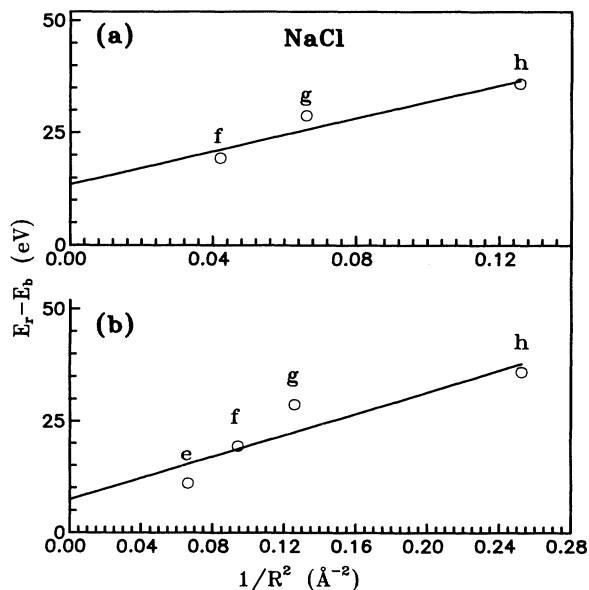


FIG. 5. Examples of unsatisfactory alternative correlations for chlorine L -edge XANES of NaCl: (a) d_{111} excluded; (b) d_{220} included; see text and Fig. 3.

D. Comparison of XANES spectra of crystalline Ar and KCl

The crystal structure of argon (around 20 K) is fcc with a unit-cell parameter of 3.57 Å,^{26,27} and the solid is isoelectronic with KCl. The *L*-edge XANES spectra of Ar in both solid and gas phases have been reported in the literature.^{27,28} Figures 6(b) and 6(a) show the digitized XANES spectrum of crystalline Ar (at 20 K (Ref. 27) along with that of KCl (at room temperature). In order to compare features of both spectra on a common scale, the energy scales have been arbitrarily set to zero at the position of peak *a*. One then finds great similarity between the two spectra. Almost all the features in the Ar spectrum correspond to features in the KCl spectrum. From comparison between *L*-edge absorption spectra of Ar in the gas and solid phases, Haensel *et al.*^{27,28} and Bianconi¹⁷ concluded that peak *a* was attributable to a $2p \rightarrow 4s$ exciton and peak *b* to a $2p \rightarrow 3d$ exciton. Similarly, we conclude, as has been suggested before,^{3,5,29} that peaks *a* and *b* in the KCl spectrum have a similar origin.

Figure 6(c) also shows the correlation plot for crystalline Ar. Although both solids have fcc lattices, the structure of Ar is Al-type (like Cu) and that of KCl is NaCl-type. Consequently, in the Ar spectrum, the resonance associated with the d_{111} lattice spacing is at a higher energy than that for the first interatomic distance; thus peak *g* is assigned to d_{111} . In the energy versus $1/R^2$ plot, the intercept with the *y* axis is close to the energy

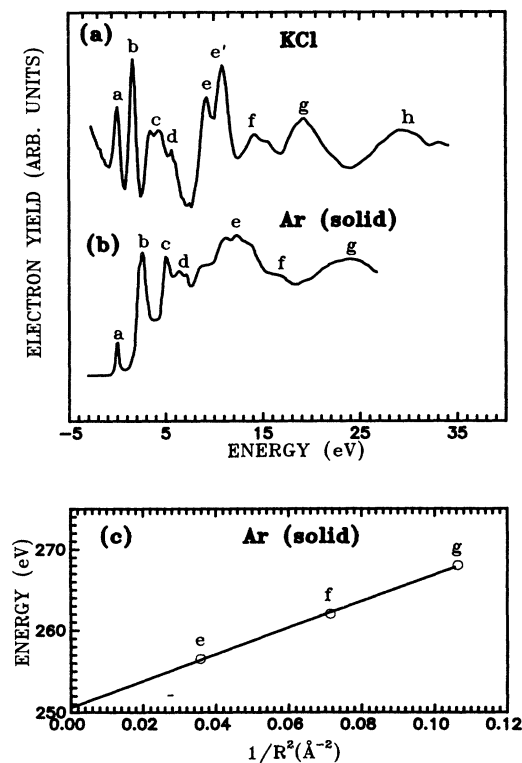


FIG. 6. Comparison of *L*-edge XANES spectrum of crystalline Ar and KCl: (a) Cl spectrum in KCl; (b) Ar spectrum (from Ref. 27); (c) correlation plot between energy and $1/R^2$ for Ar.

value of peak *b* in the Ar spectrum, which is in good agreement with the model. Energies and distances for the correlation are compared with data for alkali chlorides in Table II.

E. EXAFS contribution to XANES

Since the interatomic distances in alkali chlorides are comparatively large, one may speculate that EXAFS features might overlap with the XANES spectral region. To investigate this possibility, a theoretical Cl *L*-edge EXAFS spectrum was calculated digitally,¹⁵ using the usual EXAFS formalism³⁰ and curved wave phase functions.³¹ Interatomic distances are taken from Table II. The results for sodium chloride are shown in Figs. 7(a)–7(c). Spectrum (c) is obtained when only the first shell is included in the calculation. In spectra (b) and (a), the second and the third shell contributions in EXAFS, respectively, have been combined with the first shell. When the second shell is included in the calculations the amplitude intensity increases by a factor of ~ 6.0 . This is not unexpected, because there are 12 Cl atoms involved in the second shell and Cl has a greater scattering efficiency for electrons than Na. It seems that the effect of the $1/R^2$ coefficient in the EXAFS formalism is not large enough to offset the rise in amplitude.

As Fig. 7 shows, the width of the oscillation due to the first shell is so wide that it covers the entire range of the XANES region. When other shells are included in the calculation [Figs. 7(a) and 7(b)], some peaks are folded back in the XANES region but they are still very broad. If we compare these spectra with the experimental Cl *L*-

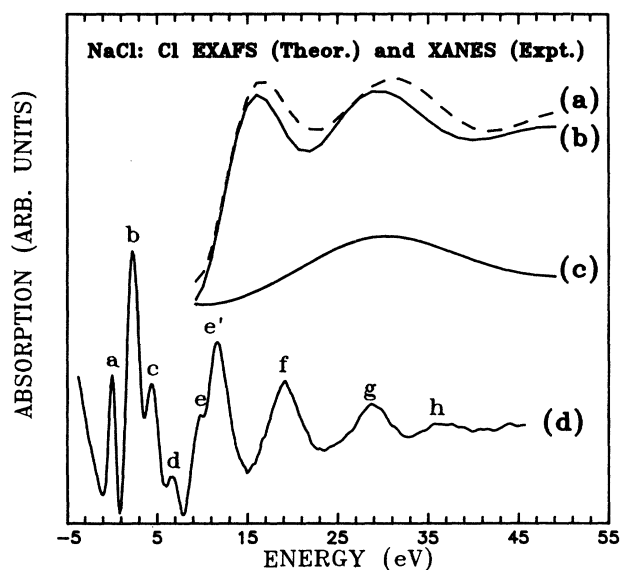


FIG. 7. Comparison of calculated chlorine *L*-edge EXAFS and experimental chlorine *L*-edge XANES in NaCl: (a) combined effects of first, second, and third shells in EXAFS calculations; (b) combined effects of first and second shells in EXAFS calculations; (c) effects of the first shell alone in EXAFS calculations; (d) Cl *L*-edge XANES experimental spectrum.

edge XANES spectra, Fig. 1(d), we notice that none of the peaks in the theoretical EXAFS spectra correspond to the observed features. However, in the absence of any absolute value for EXAFS's intensity it is very hard to speculate on the contribution (if any) of EXAFS in the XANES region.

F. Mixed crystal of NaCl and KCl

Chlorine *L*-edge XANES in mixed crystals of NaCl-KCl and KCl-RbCl have been studied by Watanabe⁵ at liquid-nitrogen temperature. He observed that the position of the first peak shifted systematically toward the lower-energy end of the spectrum as the concentration of RbCl increased in the solid solution. Also, the spectral features seemed to follow a pattern consistent with a real solid solution. On the other hand the profiles of spectra of NaCl-KCl solid solutions varied in a complicated manner, and in contrast to the KCl-RbCl composition, the position of the first peak changed in a nonlinear fashion with concentration. These observations may imply that the NaCl-KCl solid solutions were not stable under the conditions of investigation (see below). Murata *et al.*³² have investigated the Na *K*-edge XANES and EXAFS in mixed NaCl-KCl compositions at room temperature and 35 K. From their EXAFS analysis, they concluded that the distance of the first shell surrounding Na⁺ is insensitive to the presence of the K⁺ in the solid solution and has a value close to the pure NaCl lattice. This conclusion is consistent with the work of Ohno³³ who was unable to find particles with a single phase in mixtures of NaCl-KCl employing transmission electron microscopy.

Solid solutions of NaCl-KCl were prepared in the manner described in the experimental section. X-ray-diffraction analysis showed that if an ingot was either

crushed or exposed to air the single (homogeneous) phase, unmixed to the pure end-member constituents. However, ingots were apparently stable (from x-ray-diffraction analysis) for at least one week if kept in vacuum. As an example, we show in Fig. 8(a) the TEY *L*-edge XANES spectrum of 50 mol. % NaCl-KCl solid solution as compared with the spectrum of 50 mol. % mechanically mixed NaCl-KCl powders [Fig. 8(b)]. It is evident that the two spectra are identical in all respects, indicating that the original single-phase solid solution has unmixed. The apparent contradiction between the x-ray diffraction and TEY results may be explained as follows. The total electron yield method is basically a surface technique and samples to a depth of only ~ 40 Å, whereas x-ray diffraction is a bulk technique. As indicated above, unmixing is promoted on exposure to air. This suggests that the process starts on the surface. Although the samples were kept in vacuum before analysis, it was not possible to analyze them immediately after preparation. The samples were prepared in advance and transferred to the synchrotron ring only after 3–4 days in sealed evacuated tubes. Therefore residual air and/or moisture in the vacuum system coupled with aging effects were sufficient to unmix the surface layer of the samples which in agreement with the electron microscopy observation.³³ In conclusion, although in principle it may be possible to preserve true solid solutions of NaCl-KCl at room temperature in the absence of air and moisture, the surface seems to be too sensitive to remain pristine for TEY spectroscopy. A more elaborate procedure is required to produce the solid solutions *in situ*. KCl-RbCl is a better candidate for this type of investigation but because of the interference of the Rb $M_{2,3}$ edge (~ 240 eV)

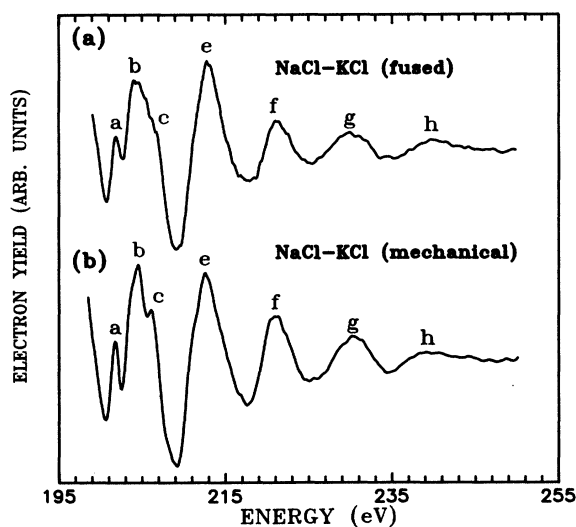


FIG. 8. Chlorine *L*-edge XANES spectra: (a) spectrum of solid solution with 50 mol. % NaCl and KCl; (b) spectrum of mechanical mixture with 50 mol. % NaCl and KCl.

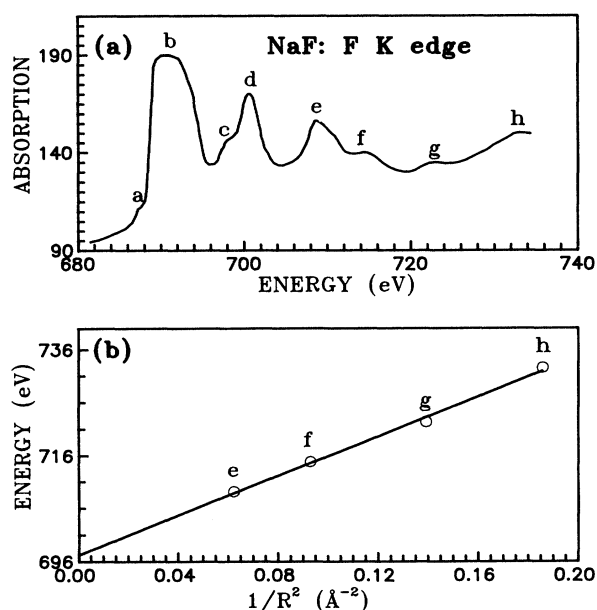


FIG. 9. (a) Fluorine *K*-edge XANES spectrum in NaF (from Ref. 34) and (b) correlation plot between energy and $1/R^2$ for NaF.

with the Cl L -edge region, this system could not be investigated effectively.

G. Interatomic-distance correlation and K edge of alkali halides

So far we have concentrated on the L edges for the correlation of post-edge features in XANES spectra. It would be of great interest to investigate the validity of the $1/R^2$ correlation for K -edge XANES spectra in alkali halides. For this investigation we make use of recent data in the literature and consider the F K -edge and Na K -edge XANES spectra in alkali halides.

High-resolution F K -edge XANES spectra in alkali fluorides (LiF to RbF) have been reported by Nakai *et al.*³⁴ For reasons which are not clear to us, some features in LiF and RbF spectra are not well resolved. Therefore we make use of only the NaF and KF XANES spectra. Figures 9(a) and 10(a) show the digitized spectra³⁴ of the K edge in NaF and KF. The peak labels are taken from the original study and we will consider only the post-edge features. As in the case of L -edge spectra, peaks e – h are correlated with interatomic distances. Since we are not certain of the value of E_b , the energy values of the features are used directly and E_b is given by the intercept of the correlated fit with the y axis. Figures 9(b) and 10(b) show the corresponding plots of energy positions versus $1/R^2$ for NaF and KF, respectively, and Table III summarizes the correlated and calculated values. Clearly, the energy-distance correlation is extremely good and the observed interatomic distances and calculated values agree within 0.1 Å. The C values calculated from the slope of the plots for NaF and KF are 187 and 292, respectively.

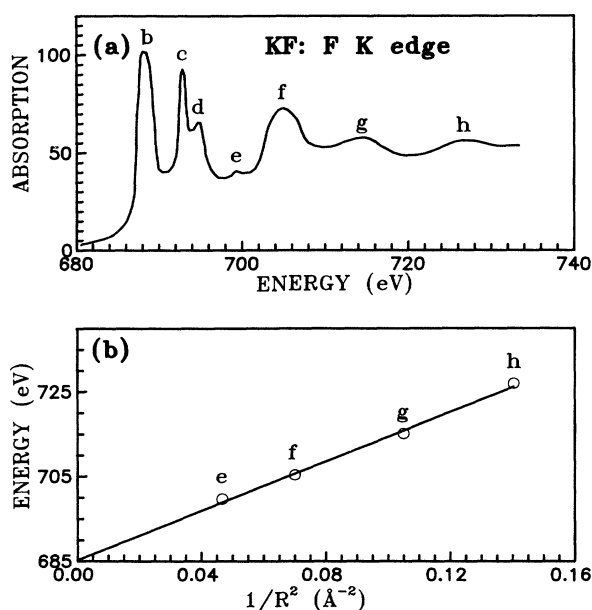


FIG. 10. (a) Fluorine K -edge XANES spectrum in KF (from Ref. 34) and (b) correlation plot between energy and $1/R^2$ for KF.

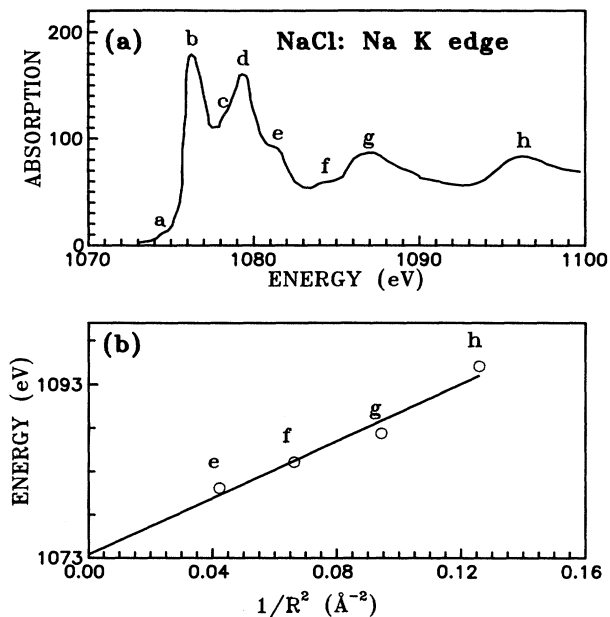


FIG. 11. (a) Sodium K -edge XANES spectrum in NaCl (from Refs. 11 and 32) and (b) correlation plot between energy and $1/R^2$ for NaCl.

In the same manner, data for Na K -edge XANES spectra from the literature have been used to investigate the interatomic-distance correlation. Figures 11(a) and 12(a) show the digitized spectra and Figures 11(b) and 12(b) demonstrate the correlation plots for NaCl (Refs. 11 and

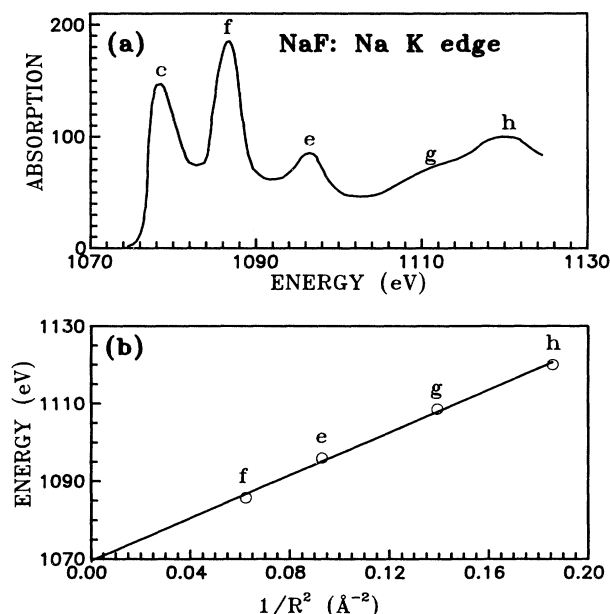


FIG. 12. (a) Sodium K -edge XANES spectrum in NaF (from Ref. 34) and (b) correlation plot between energy and $1/R^2$ for NaF.

TABLE III. Peak assignments and interatomic distances for K edges.

Shell	Peak	E_r (eV)	R (Å) Calc.	R (Å) Present
NaF (F K edge)				
R_1	h	732.5	2.32	2.30
d_{111}	g	722.3	2.68	2.73
R_2	f	714.8	3.28	3.26
R_3	e	709.1	4.01	3.88
KF (F K edge)				
R_1	h	726.8	2.67	2.64
d_{111}	g	715.0	3.09	3.13
R_2	f	705.2	3.78	3.82
R_3	e	699.5	4.63	4.51
NaCl (Na K edge)				
R_1	h	1095.0	2.82	2.79
d_{111}	g	1087.3	3.26	3.45
R_2	f	1084.0	3.89	3.92
R_3	e	1081.0	4.88	4.61
NaF (Na K edge)				
R_1	h	1120.0	2.32	2.33
d_{111}	g	1108.0	2.68	2.76
R_2	f	1096.0	3.28	3.22
R_3	e	1085.0	4.01	4.21

32) and NaF,³⁴ respectively. As in the case for the F K -edge spectra, the E_b value is found from the intercept of the plot with the y axis. In general, E_b values are close to the ionization thresholds for fluorine and sodium. The binding energies of elemental F and Na are 697 and 1071 eV, respectively. As Table III indicates the agreement between the observed and calculated values is very good.

H. General discussion

The present study has demonstrated the applicability of the energy versus $1/R^2$ correlation to the XANES spectra of simple crystalline materials. When R includes both neighbor-shell interatomic distances and the target crystal lattice spacings (d_{hkl}), all significant peaks in the post-edge region of these XANES spectra are accounted for as single-scattering resonances. Although we appreciate that the backscattering of photoelectrons in this energy region must be complex, we suggest that a successful theory for the post-edge XANES region will incorporate the present interatomic-distance correlation (as modified by inclusion of d_{hkl} spacings), and will be dominated by single-scattering processes.

The present small deviations from the energy versus $1/R^2$ correlation are attributable to experimental error (principally to error in measurement of incompletely resolved spectral features) and do not appear to have any bearing on the physical processes involved. As noted above, deviation of the constant C from the free-electron value is logically related to change in the phase shift during backscattering.

In the absence of an appropriate theoretical framework, the present approach to interpretation of the post-edge XANES region is limited to relatively simple crystalline and amorphous materials. However, the spectra of unknown materials can be fitted by trial and error. The real value of this study is that it may prove helpful to the derivation of a post-edge XANES theory and, in further demonstrating the backscattering of photoelectrons by crystal lattice planes, may lead to an improved understanding of electron backscattering processes in solids.

IV. CONCLUSIONS

We conclude with the following statements.

(i) The post-edge region of Cl L -edge XANES spectra in the alkali chlorides is extremely sensitive to interatomic-distance variation of the nearest as well as long-range neighbors of the Cl^- ion. The positions of absorption peaks have been correlated with $1/R^2$, where R is the interatomic distance.

(ii) The largest lattice spacings (d_{hkl}) have to be included in the correlation to account for all the major peaks in the post-edge region.

(iii) Mixed crystals of NaCl-KCl are not stable in air and, in particular, surface layers unmix very rapidly. More elaborate experimental arrangements are required to collect TEY spectra of these solid solutions. All the previous studies have been performed on thin films in the absorption mode.^{5,32}

(iv) The $1/R^2$ rule has also been extended to the F K edge and the Na K edge in alkali halides.

(v) The theoretical framework for the correlation with $1/R^2$, and specially for the resonances associated with lattice spacings, is unclear. Further theoretical and experimental work is in progress.

ACKNOWLEDGMENTS

The authors are grateful to T. Tyliczszak for use of his computer program and J. D. Bozek for his assistance with software development. We also thank the staff at the Synchrotron Radiation Centre, University of Wisconsin for their technical support. This study was financially supported by the Natural Sciences and Engineering Research Council and the National Research Council of Canada.

¹T. Sagawa, Y. Iguchi, M. Sasanuma, T. Nasu, S. Yamaguchi, S. Fujiwara, M. Nakamura, A. Ejiri, T. Masuoka, T. Sasaki, and T. Oshio, J. Phys. Soc. Jpn. **21**, 2587 (1966).

²Y. Iguchi, T. Sagawa, S. Sato, M. Watanabe, H. Yamashita, A. Ejiri, M. Sasanuma, S. Nakai, M. Nakamura, S. Yamaguchi,

Y. Nakai, and T. Oshio, Solid State Commun. **6**, 575 (1968).

³O. Aita, I. Nagakura, and T. Sagawa, J. Phys. Soc. Jpn. **30**, 1414 (1971).

⁴F. C. Brown, C. Gähwiller, H. Fujita, A. B. Kunz, W. Scheifley, and N. Carrera, Phys. Rev. B **2**, 2126 (1970).

- ⁵M. Watanabe, *J. Phys. Soc. Jpn.* **34**, 755 (1973).
- ⁶S. T. Pantelides and F. C. Brown, *Phys. Rev. Lett.* **33**, 298 (1974); S. T. Pantelides, *Phys. Rev. B* **11**, 2391 (1975).
- ⁷A. B. Kunz, *Phys. Rev.* **175**, 1147 (1968).
- ⁸A. B. Kunz, *Phys. Rev. B* **26**, 2056 (1982) and references therein.
- ⁹F. J. Himpsel and W. Steinman, *Phys. Rev. B* **17**, 2537 (1978).
- ¹⁰R. V. Vedrinskii, L. A. Bugaev, I. I. Gegusin, V. L. Kraizman, A. A. Novakovich, S. A. Prosandeev, R. E. Ruus, A. A. Maiste, and M. A. Elango, *Solid State Commun.* **44**, 1401 (1982).
- ¹¹T. Fujikawa, T. Okazawa, K. Yamasaki, J.-C. Tang, T. Murata, T. Matsukawa, and S. Naoe, *J. Phys. Soc. Jpn.* **58**, 2952 (1989).
- ¹²M. Kasrai, M. E. Fleet, T. K. Sham, G. M. Bancroft, K. H. Tan, and J. R. Brown, *Solid State Commun.* **68**, 507 (1988).
- ¹³W. T. Barrett and W. E. Wallace, *J. Amer. Chem. Soc.* **76**, 355 (1954).
- ¹⁴G. M. Bancroft, K. H. Tan, and J. D. Bozek, *Phys. Canada*, July 113 (1987).
- ¹⁵T. Tyliczszak (unpublished).
- ¹⁶G. M. Bancroft, J. D. Bozek, J. N. Cutler, and K. H. Tan, *J. Electron Spectrosc. Relat. Phenom.* **47**, 187 (1988).
- ¹⁷A. Bianconi, in *X-ray Absorption: Principle, Applications, Techniques of EXAFS and XANES*, edited by D. C. Koningsberger and R. Prins (Wiley, New York, 1988), p. 573.
- ¹⁸F. W. Lytle, *Ber. Bunsenges. Phys. Chem.* **91**, 1251 (1987); F. W. Lytle, R. B. Gregor, and A. J. Panson, *Phys. Rev. B* **37**, 1550 (1988).
- ¹⁹J. C. Hermanson, *Phys. Rev.* **177**, 1234 (1969).
- ²⁰R. Haensel, G. Keitel, P. Schreiber, and C. Kunz, *Phys. Rev.* **188**, 1375 (1969).
- ²¹C. R. Natoli, in *EXAFS and Near Edge Structure*, Vol. 27 of *Springer Series in Chemical Physics*, edited by A. Bianconi, L. Incoccia, and S. Stipcich (Springer, Berlin, 1983), p. 43; in *EXAFS and Near Edge Structure III*, edited by K. O. Hodgson, B. Hedman, and J. E. Penner-Hahn (Springer-Verlag, Berlin, 1984), p. 38.
- ²²A. Bianconi, E. Fritsch, G. Calas, and J. Petiau, *Phys. Rev. B* **32**, 4292 (1985).
- ²³J. S. Tse, *J. Chem. Phys.* **89**, 920 (1988).
- ²⁴L. W. Finger, Computer program BADTEA, University of Minnesota, Minneapolis (1968).
- ²⁵D. A. L. Kilcoyne, C. McCarthy, S. Nordholm, N. S. Hush, and P. R. Hilton, *J. Electron Spectrosc. Relat. Phenom.* **36**, 153 (1985).
- ²⁶G. L. Pollack, *Rev. Mod. Phys.* **36**, 748 (1964).
- ²⁷R. Haensel, G. Keitel, N. Kosuch, U. Nielsen, and P. Schreiber, *J. Phys. (Paris) Colloq.* **32**, C4-236 (1971).
- ²⁸R. Haensel, G. Keitel, E. E. Koch, M. Skibowski, and P. Schreiber, *Phys. Rev. Lett.* **15**, 1160 (1969).
- ²⁹F. C. Brown, in *Synchrotron Radiation Research*, edited by H. Winick and S. Doniach (Plenum, New York, 1980), p. 61.
- ³⁰P. A. Lee, P. H. Citrin, P. Eisenberger, and B. M. Kincaid, *Rev. Mod. Phys.* **53**, 769 (1981).
- ³¹A. G. Mckale, B. W. Veal, A. P. Paulikas, S. K. Chan, and G. S. Knapp, *J. Am. Chem. Soc.* **110**, 3763 (1988).
- ³²T. Murata, T. Matsukawa, and S. Naoe, *Solid State Commun.* **66**, 787 (1988).
- ³³T. Ohno, *J. Cryst. Growth* **73**, 263 (1985).
- ³⁴S. Nakai, M. Ohashi, T. Mitsuishi, H. Maezawa, H. Oizumi, and T. Fujikawa, *J. Phys. Soc. Jpn.* **55**, 2436 (1986).